European Neuropsychopharmacology (2019) 29, 278–290

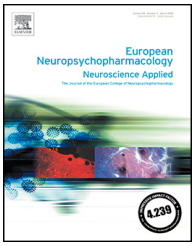

www.elsevier.com/locate/euroneuro

In vivo metabotropic glutamate receptor 5 availability-associated functional connectivity alterations in drug-naïve young adults with major depression

Jong-Hoon Kim[a,b,c,*], **Yo-Han Joo**[b], **Young-Don Son**[b,c,d], **Jeong-Hee Kim**[b,e], **Yun-Kwan Kim**[b], **Hang-Keun Kim**[b,c,d], **Sang-Yoon Lee**[b,c,f], **Tatsuo Ido**[b]

[a] *Department of Psychiatry, Gil Medical Center, Gachon University College of Medicine, Gachon University, 1198 Guwol-dong, Namdong-gu, Incheon 405-760, South Korea*
[b] *Neuroscience Research Institute, Gachon University, Incheon, South Korea*
[c] *Gachon Advanced Institute for Health Science and Technology, Graduate School, Gachon University, Incheon, South Korea*
[d] *Department of Biomedical Engineering, College of Health Science, Gachon University, Incheon, South Korea*
[e] *Research Institute for Advanced Industrial Technology, Korea University, Sejong, South Korea*
[f] *Department of Neuroscience, Gachon University College of Medicine, Gachon University, Incheon, South Korea*

Received 23 April 2018; received in revised form 20 November 2018; accepted 1 December 2018

KEYWORDS
Metabotropic glutamate receptor-5; Positron emission tomography; [^{11}C]ABP688; Functional magnetic resonance imaging; Major depression

Abstract
There has been increasing interest in glutamatergic neurotransmission as a putative underlying mechanism of depressive disorders. We performed [^{11}C]ABP688 positron emission tomography (PET) and resting-state functional magnetic resonance imaging (rs-fMRI) in drug-naïve young adult patients with major depression to examine alterations in metabotropic glutamate receptor-5 (mGluR5) availability, and to investigate their functional significance relating to neural systems-level changes in major depression. Sixteen psychotropic drug-naïve patients with major depression without comorbidity (median age: 22.8 years) and fifteen matched healthy controls underwent [^{11}C]ABP688 PET imaging and 3-T MRI. For mGluR5 availability,

* Corresponding author at: Department of Psychiatry, Gil Medical Center, Gachon University College of Medicine, Gachon University, 1198 Guwol-dong, Namdong-gu, Incheon 405-760, South Korea.
E-mail address: jhnp@chol.com (J.-H. Kim).

https://doi.org/10.1016/j.euroneuro.2018.12.001

we quantified [^{11}C]ABP688 binding potential (BP_{ND}) using the simplified reference tissue model. Seed-based functional connectivity analysis was performed using rs-fMRI data with regions derived from quantitative [^{11}C]ABP688 PET analysis as seeds. In region-of-interest (ROI)-based and voxel-based analyses, the [^{11}C]ABP688 BP_{ND} was significantly lower in patients than in controls in the prefrontal cortex ROI and in voxel clusters within the prefrontal, temporal, and parietal cortices, and supramarginal gyrus. The [^{11}C]ABP688 BP_{ND} seed-based functional connectivity analysis showed significantly less negative connectivity from the inferior parietal cortex seed to the fusiform gyrus and inferior occipital cortex in patients than in controls. The correlation patterns between [^{11}C]ABP688 BP_{ND} and functional connectivity strength (β) for the superior prefrontal cortex seed were opposite in the depression and control groups. In conclusion, using a novel approach combining [^{11}C]ABP688 PET and rs-fMRI analyses, our study provides a first evidence of lower mGluR5 availability and related functional connectivity alterations in drug-naïve young adults with major depression without comorbidity.

1. Introduction

Recent years have seen increasing interest in glutamatergic neurotransmission, both as a putative underlying mechanism of depressive disorders, and as an emerging target for novel antidepressant treatments (Sanacora et al., 2012; Abdallah et al., 2015, 2016). The most compelling evidence for a glutamate hypothesis of depression has come from clinical studies showing rapid-acting antidepressant and anti-suicidal effects of ketamine, an uncompetitive N-methyl-D-aspartic acid (NMDA) receptor antagonist (Zarate et al., 2006; Singh et al., 2016; Sanacora et al., 2017). While NMDA receptors mediate rapid signaling via glutamate-gated cation channels, the metabotropic glutamate receptors (mGluRs) modulate synaptic transmission through G-protein-coupled intracellular signaling pathways, and influence NMDA receptor-mediated neurotransmission. The mGluRs have also been implicated in the pathophysiology of depression, particularly the mGluR5 subtype, which is highly expressed in the neocortex and hippocampus (Chaki et al., 2013; Esterlis et al., 2017). Functional and mechanistic links of mGluR5 signaling to NMDA receptor-related complexes, such as Homer, Shank, and postsynaptic density-95, are considered key aspects of mGluR5 signaling in relation to the glutamate hypothesis of depression (Tu et al., 1999; Chaki et al., 2013). The functional relationships of mGluR5 with brain-derived neurotrophic factor (Legutko et al., 2006) and serotonergic signaling (Bradbury et al., 2003; Smolders et al., 2008) also present potential mechanisms linking mGluR5 with depression. Preclinical studies have reported that antagonists or negative allosteric modulators of mGluR5 show some antidepressant effects in animal models of depression (Tatarczyńska et al., 2001; Li et al., 2006; Belozertseva et al., 2007) and that mGluR5 knockout mice have a behavioral phenotype congruent with antidepressant-like effects (Li et al., 2006). These findings support the involvement of mGluR5 in the pathophysiological process of depression.

However, direct *in vivo* evidence that mGluR5 is involved in depression in the human brain is lacking. The study by Deschwanden et al. (2011) examined mGluR5 availability using [^{11}C]ABP688 PET in 11 middle-aged patients with major depression, and observed significantly lower levels of mGluR5 availability in patients than in controls in the prefrontal cortex, which was confirmed in a postmortem investigation of mGluR5 protein expression using an independent sample of human postmortem tissue. Another [^{11}C]ABP688 PET study by DeLorenzo et al. (2015) reported no deficit in mGluR5 availability in 20 patients with late-life major depression. A recent publication by Abdallah et al. (2017) using [^{18}F]FPEB PET reported no significant alterations in mGluR5 volume of distribution in 30 medication-free patients with major depression.

The previous equivocal mGluR5 PET findings in depression could reflect inhomogeneity of subject groups with respect to potential confounding factors, such as age distribution, history of antidepressant use, or comorbidity with anxiety disorders. To our knowledge, no studies have examined mGluR5 availability in a homogeneous group of medication-naïve young adults suffering from major depression without comorbidity. Although the prevalence of depression and risk of suicide in subjects in their 20 s is particularly alarming (Ibrahim et al., 2013), the underlying neurobiological correlates of depression in this cohort remain poorly characterized. Depression in patients in their 20 s has a high rate of under-recognition, which can lead to a serious accumulation of negative consequences owing to the influence on careers and social relationships (Aalto-Setälä et al., 2001). Therefore, investigation into glutamatergic dysregulation as an underlying neurochemical mechanism for young adult depression is justified.

On the other hand, previous resting-state functional magnetic resonance imaging (rs-fMRI) studies have shown both increased (Zhou et al., 2010; Hwang et al., 2016; Kaiser et al., 2016) and decreased (Anand et al., 2005; Liu et al., 2012; Guo et al., 2013) functional connectivity to be associated with major depression. These varying results may stem from different seed regions and population characteristics. Given the glutamatergic basis of the fMRI signals crucial for cerebral functioning (Hyder et al., 2001; Kida and Hyder, 2006), we can infer that changes in glutamate receptor availability may ultimately be related to systems-level changes in neural circuitry (Abi-Dargham and Horga, 2016), such that the foci of altered mGluR5 availability in the cerebral cortex could lead to perturbed functional connectivity with distal regions. Combining molecular PET

imaging with a specific mGluR5 ligand and rs-fMRI measuring connectivity can be useful for gaining insights into the functional significance of altered mGluR5-mediated neurotransmission.

Therefore, the purpose of this study was to quantify *in vivo* mGluR5 availability using PET with [^{11}C]ABP688, a radioligand that binds to an allosteric site on mGluR5, in drug-naïve young adult patients with major depression without comorbidity as well as in matched healthy controls. The goal was to examine whether there are significant alterations in mGluR5 availability in the patient group. To examine the functional significance of possible alterations in mGluR5 availability, we also performed rs-fMRI in the same subjects, and conducted functional connectivity analyses using rs-fMRI data with regions derived from quantitative PET analysis as seeds. In the PET investigation, we hypothesized that mGluR5 availability would be lower in the prefrontal cortex in patients than in matched controls. The prefrontal cortex was chosen *a priori* based on previous *in vivo* PET and post-mortem investigations (Deschwanden et al., 2011) and on additional literature implicating the prefrontal cortex in the glutamatergic mechanisms underlying depression (Duman, 2014; Abdallah et al., 2016; Chowdhury et al., 2017).

2. Experimental procedures

2.1. Participants

The study protocol was approved by the Institutional Review Board of the Gachon University Gil Medical Center, and all procedures used in the study were conducted in accordance with international ethical standards and the Declaration of Helsinki. Written informed consent was obtained from all participants after a full explanation of the study procedures. Since our study was focused on elucidating the neurobiological correlates in a homogeneous group of drug-naïve young adult patients in their 20 s, the first inclusion criterion was (i) age from 19 (legal adult age in South Korea) to 29 years. Other inclusion criteria were; (ii) diagnosis of major depressive disorder by the Diagnostic and Statistical Manual of Mental Disorders 4th edition (DSM-IV) (American Psychiatric Association, 1994), which was established using the Structured Clinical Interview for DSM-IV (SCID-IV) (First et al., 1996), with no other current Axis I diagnosis. In particular, patients with major depression and comorbid anxiety disorders, e.g., generalized anxiety disorder, panic disorder, social phobia, obsessive-compulsive disorder, or posttraumatic stress disorder, were excluded; (iii) no past or current substance abuse/dependence (nicotine use was allowed); (iv) no history of medical or neurological disorders; and (v) no past or current use of psychotropic medications (such as antidepressants, benzodiazepines/anxiolytics, hypnotics, antipsychotics, or mood stabilizers). Sixteen patients meeting these criteria were enrolled and completed the study (Table 1). The patients' mean age was 23.4 $\pm$ 2.8 (median: 22.8) years and duration of current episode of depression was 7.8 $\pm$ 6.8 (median: 6.0) months. To compare neuroimaging findings between patients with major depression and healthy subjects, 15 matched healthy controls, who met the criteria of no past or current psychiatric, neurological, or medical disorders, and no past or current use of medications known to affect the central nervous system (except for nicotine use), were recruited, provided written informed consent, and underwent the same PET and rs-fMRI protocols. None of the participants showed any structural abnormalities on brain MRI, which was confirmed by a board-certified radiologist. Patients were recruited from outpatient clinics and through local advertisements, and control subjects were recruited through local advertisements.

2.2. Clinical assessments

Clinical assessments were conducted using the Beck Depression Inventory (BDI) (Beck, 1967), Hamilton Rating Scale for Depression (HAMD-17) (Hamilton, 1960), Beck Hopelessness Scale (BHS) (Beck et al., 1974), and Rosenberg Self-Esteem Scale (RSES) (Rosenberg, 1965). For the HAMD-17, BDI, and BHS, higher scores indicate more severe symptoms, whereas higher RSES scores indicate greater self-esteem. The patients' mean HAMD-17 score was 19.6 $\pm$ 6.1 (range: 12–29; Table 1). Based on the severity classification on the HAMD-17 (Zimmerman et al., 2013), five patients were rated as having mild severity, five as having moderate severity, and six as having severe depression.

2.3. Scan protocol for [^{11}C]ABP688 PET imaging

All participants were scanned using a Biograph 6 PET scanner (Siemens Medical Imaging Systems, Knoxville, USA) with [^{11}C]ABP688. All PET scans were performed at the same time of the day (10:00 a.m.) to avoid possible diurnal variations in glutamate levels that may affect mGluR5 surface localization and ligand accessibility (DeLorenzo et al., 2011a, 2017). The tracer [^{11}C]ABP688 was synthesized as previously described (Ametamey et al., 2006). Following bolus injection of a mean dose of 636.2 $\pm$ 71.4 MBq [^{11}C]ABP688 with a mean specific activity of 17.8 $\pm$ 6.5 GBq/μmol, a dynamic emission recording lasting 60 min was initiated in list mode. A computed tomography (CT)-based transmission scan was performed immediately prior to the tracer injection and used to estimate attenuation of the PET data. The [^{11}C]ABP688 PET images were reconstructed using the 2-dimensional ordered-subset expectation maximization (OSEM-2D) algorithm. The reconstructed PET images had a matrix size of 256 $\times$ 256 $\times$ 109 and a voxel size of 1.33 $\times$ 1.33 $\times$ 1.50 mm^3. To calculate the [^{11}C]ABP688 binding potential with respect to non-displaceable compartment (BP_{ND}), the emission data of [^{11}C]ABP688 PET were reconstructed into 21 frames of the following duration: 2 $\times$ 15 s, 3 $\times$ 30 s, 3 $\times$ 60 s, 2 $\times$ 90 s, 3 $\times$ 120 s, 2 $\times$ 180 s, 4 $\times$ 300 s, and 2 $\times$ 600 s (total 60 min). Attenuation, scatter, and decay time correction were estimated and applied for each frame.

2.4. Scan protocol for resting-state fMRI

The 3-T MRI (Magnetom Verio; Siemens, Erlangen, Germany) scans were performed using a 3-dimensional T1-weighted magnetization-prepared rapid gradient echo (3-D T1MPRAGE) sequence for structural brain imaging. The 3-D T1MPRAGE images were acquired with the following parameters: repetition time = 1900 ms, echo time = 3.3 ms, inversion time = 900 ms, flip angle = 9°, voxel size = 0.5 $\times$ 0.5 $\times$ 1.0 mm^3, matrix size = 416 $\times$ 512, and number of slices = 160.

For rs-fMRI recordings optimized for detecting changes in blood oxygen level- dependent (BOLD) signal levels, the 3-T rs-fMRI images were acquired using echo planar imaging (EPI) with the following parameters: repetition time = 3000 ms, echo time = 30 ms, flip angle = 90°, pixel size = 3.5 $\times$ 3.5 mm^2, thickness = 3.5 mm, matrix size = 72 $\times$ 72, and number of slices = 45. We used a twelve-channel transmit-and-receive radiofrequency phase array head coil (iPAT, Siemens, Erlangen, Germany). A total of 180 volumes (nine minutes in length) were acquired for each subject's rs-fMRI session. All subjects were instructed to relax, lie still, and stay awake in the scanner, with their head movement comfortably restricted by sponges.

Table 1 Demographic/clinical characteristics and PET scan parameters.

Variables	Patients ($N = 16$)	Controls ($N = 15$)	p-value
Age (years)	23.4 ± 2.8	24.7 ± 3.1	0.241
Gender (male/female)	7/9	9/6	0.367
Smoker/nonsmoker	3/13	1/14	0.316
Number of cigarettes smoked (per day)	1.8 ± 4.0	0.3 ± 1.3	0.173
Duration of current episode (months)	7.8 ± 6.8	-	-
Age of onset (years)	21.7 ± 2.5	-	-
HAMD-17	19.6 ± 6.1	-	-
Range of HAMD-17 score	12–29	-	-
BDI	24.0 ± 7.2	0.8 ± 1.1	<0.001
BHS	10.5 ± 5.4	1.5 ± 1.6	<0.001
RSES	23.0 ± 5.5	33.4 ± 4.5	<0.001
Injected dose (MBq)	647.21 ± 45.20	625.14 ± 90.90	0.407
Specific activity (GBq/umol)	18.19 ± 5.10	17.45 ± 7.79	0.786

HAMD, Hamilton Rating Scale for Depression; BDI, Beck Depression Inventory; BHS, Beck Hopelessness Scale; RSES, Rosenberg Self-Esteem Scale.

2.5. Image analysis

2.5.1. [^{11}C]ABP688 PET imaging

The 3-D T1MPRAGE MRI images of each subject were coregistered to PET images using Statistical Parametric Mapping 12 (SPM12; Wellcome Trust Center for Neuroimaging, UK). The coregistered MRI images were spatially normalized to the Montreal Neurological Institute (MNI) template using SPM12 with the nonlinear deformation field, and the estimated transform was applied to the corresponding PET images. Time-activity curves of [^{11}C]ABP688 PET were generated from dynamic PET images by averaging all the voxels within each region of interest (ROI), which were coregistered to the corresponding MRI images. For estimating mGluR5 availability, [^{11}C]ABP688 BP_{ND} was derived from each ROI using the simplified reference tissue model 2 (SRTM2) (Wu and Carson, 2002) with cerebellar gray matter as the reference region as previously suggested for this tracer (DeLorenzo et al., 2011a, 2011b, 2015; DuBois et al., 2016), based on the parameter estimation implemented in the PMOD software v3.8 (PMOD Technologies Ltd., Zürich, Switzerland). Despite the lack of brain regions completely devoid of mGluR5, postmortem studies have reported that specific mGluR5 binding in cerebellar gray matter is negligible (Daggett et al., 1995; Berthele et al., 1999; Deschwanden et al., 2011). The cerebellar gray matter has also been validated as a suitable reference region for [^{11}C]ABP688 PET by displacement studies (Elmenhorst et al., 2010; Mathews et al., 2014). Moreover, in our study, there was no significant difference in cerebellar standard uptake value (SUV) between the depression and control groups ($p = 0.99$), nor was there any significant group difference in cerebellar gray matter volume ($p = 0.78$) (Supplementary Fig. S1). Representative examples of [^{11}C]ABP688 BP_{ND}, PET, and 3-T MR images are shown in Supplementary Fig. S2. The BP_{ND} values were obtained in the *a priori* ROI, i.e., the prefrontal cortex. The anatomical location of the prefrontal cortex was determined based on the Brodmann areas in the Talairach atlas (Lancaster et al., 2000), which includes dorsolateral prefrontal, medial prefrontal, ventrolateral prefrontal, and orbitofrontal subregions (Teffer and Semendeferi, 2012). The left and right regions were analyzed separately, since previous studies have reported functional imbalance between the left and right prefrontal cortices in depression (Martinot et al., 1990; Grimm et al., 2008; Paillère Martinot et al., 2010) and a lateralized role of the prefrontal cortex in responses to emotional stimuli (Ochsner et al., 2002). In our subjects, BP_{ND} values were higher in the right prefrontal cortex than in the left prefrontal cortex (patient group: $p = 0.016$; control group: $p = 0.011$). To perform exploratory group comparisons for regions other than the prefrontal cortex ROI, BP_{ND} values were also obtained in 12 additional bilateral regions defined using the automated anatomical labeling (AAL) program (Tzourio-Mazoyer et al., 2002). These regions were the anterior cingulate gyrus, superior temporal cortex, middle temporal cortex, inferior temporal cortex, superior parietal cortex, inferior parietal cortex, hippocampus, amygdala, thalamus, caudate, putamen, and globus pallidus. In addition, we also performed a whole-brain voxel-based analysis to further identify group differences in [^{11}C]ABP688 BP_{ND} in other brain regions.

2.5.2. [^{11}C]ABP688 BP_{ND} seed-based resting-state fMRI

Preprocessing of the MRI images was performed using SPM12. The 3-D T1MPRAGE image of each subject was segmented into gray matter, white matter, and cerebrospinal fluid (CSF) images and was coregistered to the rs-fMRI image. The segmented T1 images were spatially normalized to the MNI template and the same transform was applied to the corresponding rs-fMRI images. Both images were resampled to 2-mm isotropic voxels and smoothed by a 3D Gaussian low-pass filter at 6-mm full-width at half-maximum (FWHM).

Denoising of the rs-fMRI data was performed using linear regression to remove unwanted physiological and motion effects. The denoising steps were based on a default scheme implemented in the functional connectivity toolbox (CONN) software package (CONN v.17.f) (http://web.mit.edu/swg/software.htm; Whitfield-Gabrieli and Nieto-Castanon, 2012). The five principal components from white matter and CSF time series were extracted using the CompCor method (Behzadi et al., 2007), and the components were added as confounds in the denoising step. Realignment parameters in six degrees of freedom were also included as regressors to correct for motion, with application of bandpass filtering (0.008–0.09 Hz) and linear detrending.

To investigate the effect of alteration in mGluR5 availability on functional connectivity, we undertook seed-to-ROI analysis of the rs-fMRI data using the CONN software package. Here, the seed regions were derived from the voxel-based group comparisons of [^{11}C]ABP688 BP_{ND} (BP_{ND}-based seeds), and were based on the peak voxel coordinates, i.e., clusters with a statistical threshold of false discovery rate (FDR)-corrected $p < 0.05$. For every subject, bivariate correlations between the seeds and ROIs were used for the first-level analysis of functional connectivity. Based on the AAL atlas, 116 predefined cortical and subcortical regions were used as the target ROIs in the seed-to-ROI rs-fMRI analysis.

2.6. Statistical analysis

2.6.1. [^{11}C]ABP688 PET imaging

The mean [^{11}C]ABP688 BP_{ND} values were compared between the two groups using ROI-based and voxel-based approaches. In the prefrontal cortex ROI-based analysis, between-group comparisons were performed using analysis of covariance (ANCOVA) with the relevant variable as a covariate. Effect sizes (Cohen's d) were also calculated. A two-tailed p-value < 0.025 was defined as the threshold of statistical significance. In the voxel-based whole brain analysis with the relevant variable as a covariate, statistical significance was set at FDR-corrected $p < 0.05$ to account for multiple comparisons. The relationship between [^{11}C]ABP688 BP_{ND} and clinical severity was also examined using ROI-based and voxel-based approaches. In the prefrontal cortex ROI analysis, relationships were analyzed using Pearson's correlation coefficients. A two-tailed p-value < 0.0063 was considered significant after adjustment for multiple correlations. In the voxel-based analysis, voxel-wise linear regression analysis was conducted using spatially normalized [^{11}C]ABP688 BP_{ND} images with clinical variables as regressors, and the threshold for statistical significance was set at FDR-corrected $p < 0.05$.

2.6.2. Functional connectivity using resting-state fMRI

The [^{11}C]ABP688 BP_{ND} seed-based rs-functional connectivity was analyzed as follows. The correlations between the average time courses of the BP_{ND}-based seed to target ROIs were calculated, and Fisher's z-transformation was performed on Pearson's bivariate correlation coefficients. A two-tailed two-sample t-test was performed for the transformed values to examine group differences in seed-based rs-functional connectivity. The significance threshold was set at FDR-corrected $p < 0.05$. To examine the correlation between [^{11}C]ABP688 BP_{ND} seed-based rs-functional connectivity and clinical severity, we conducted correlation analysis with a significance level of FDR-corrected $p < 0.05$.

2.6.3. Association between mGluR5 availability and related functional connectivity

Using the CONN software, we performed a multivariate regression analysis for each subject to determine the functional connectivity strength (β map) between each seed and every target ROI after controlling for the contributions of all the other seeds. In this first-level analysis, 116 cortical and subcortical regions of the AAL atlas and 84 Brodmann areas defined in the Talairach atlas were used as the target ROIs. In the second-level analysis, linear regression analysis was conducted in each group to examine the associations between [^{11}C]ABP688 BP_{ND} for each seed and functional connectivity strength for all seed-target pairs, and the resultant T-values were acquired. Exploratory between-group comparisons of the association between [^{11}C]ABP688 BP_{ND} and functional connectivity strength were performed using the CONN software, with a significance level of uncorrected $p < 0.005$.

3. Results

The clinical characteristics of the participants are presented in Table 1. Age, gender distribution, smoking characteristics, and scan parameters did not differ between the two groups.

3.1. Between-group comparisons of mGluR5 availability

Although smoking characteristics did not differ between the groups, we performed the between-group analysis with smoking as a covariate, considering the reports that mGluR5 availability is affected by cigarette smoking (Akkus et al., 2013; Hulka et al., 2014). The ROI-based analysis using ANCOVA indicated significantly lower [^{11}C]ABP688 BP_{ND} in patients than in controls for the bilateral prefrontal cortex (right: effect size $= 1.05$, $p = 0.013$; left: effect size $= 1.09$, $p = 0.009$) (Table 2A). The ROI volumes were not different between the patient and control groups (right prefrontal cortex: 64.58 ± 6.49 cm^3 vs. 66.22 ± 8.24 cm^3, $t = -0.62$, $p = 0.54$; left prefrontal cortex: 64.91 ± 6.89 cm^3 vs. 65.97 ± 8.45 cm^3, $t = -0.39$, $p = 0.70$). Exploratory between-group comparisons of [^{11}C]ABP688 BP_{ND} values for other regions of the brain revealed lower [^{11}C]ABP688 BP_{ND} in patients than in controls, with small to large effect sizes across the regions (Supplementary Table S1). There were no significant group differences in the brain volumes of these additional ROIs ($p > 0.1$) (Supplementary Table S2).

The voxel-based whole brain analysis with smoking as a covariate revealed that [^{11}C]ABP688 BP_{ND} values were significantly lower in patients than in controls in clusters of voxels centered in the prefrontal cortex (left superior medial, left superior, left middle, and right inferior opercular regions) (FDR-corrected $p < 0.05$) (Table 2B; Fig. 1(A)). Voxel-based analysis also showed significantly lower [^{11}C]ABP688 BP_{ND} values in patients than in controls in clusters located in the temporal (left inferior, right superior/middle pole) and parietal (right inferior) cortices, and the right supramarginal gyrus (FDR-corrected $p < 0.05$) (Table 2B; Fig. 1(A)). We performed the same between-group comparisons in non-smoking participants after excluding the smokers from the analysis. The ROI-based analysis showed lower [^{11}C]ABP688 BP_{ND} values in the bilateral prefrontal cortex in patients than in controls at $p \leq 0.05$ (left: 0.40 ± 0.05 vs. 0.45 ± 0.06, $p = 0.038$; right: 0.46 ± 0.06 vs. 0.52 ± 0.07, $p = 0.050$). The voxel-based whole brain analysis also showed results similar to those observed in the entire participants. The [^{11}C]ABP688 BP_{ND} values were lower in patients than in controls in clusters located in the prefrontal, temporal, and parietal cortices, and supramarginal gyrus (uncorrected $p < 0.0001$) (Supplementary Table S3).

In the patient group, [^{11}C]ABP688 BP_{ND} values did not significantly correlate with the BDI, HAMD-17, BHS, or RSES scores in the ROI-based or voxel-based analysis. In the entire subject group (depression and control groups), the ROI-based analysis showed significant negative correlations between the BDI score and the [^{11}C]ABP688 BP_{ND} in the bilateral prefrontal cortex (left: $r = -0.49$, $p = 0.006$; right: $r = -0.47$, $p = 0.007$). The voxel-based analysis also showed significant negative correlations between the BDI score and [^{11}C]ABP688 BP_{ND} for the entire subject group (FDR-corrected $p < 0.05$) (Supplementary Table S4A; Fig. 2(A)).

3.2. [^{11}C]ABP688 BP_{ND} seed-based rs-functional connectivity

As shown in Table 2B, the clusters derived from the voxel-based between-group comparisons of [^{11}C]ABP688 BP_{ND} were located in the prefrontal, temporal, and parietal cortices, and supramarginal gyrus. As noted above, we set the peaks of these clusters as the seed regions for rs-functional connectivity analysis. Two-sample t-tests revealed

Table 2A ROI-based between-group comparisons of regional [^{11}C]ABP688 BP_{ND} values.

ROIs	[^{11}C]ABP688 BP_{ND} value		*p*-value	Effect size (Cohen's d)	ANCOVA
	Depression group Mean (SD)	Control group Mean (SD)			
Rt. prefrontal cortex	0.446 (0.074)	0.522 (0.070)	0.007	1.051	0.013
Lt. prefrontal cortex	0.384 (0.064)	0.454 (0.065)	0.005	1.088	0.009

ROI, region of interest; BP_{ND}, binding potential with respect to non-displaceable compartment; SD, standard deviation; ANCOVA, analysis of covariance; Rt, right; Lt, left.

Table 2B Voxel-based between-group comparisons of [^{11}C]ABP688 BP_{ND} values.

Patients < Controls						
Peak MNI coordinate	Regions	Cluster size	Cluster volume (mm^3)	Peak *T*-value	*p*-value (uncorr.)	FDR*p*
66; −8; 0	Rt. superior temporal cortex	46	368	5.352	0.00001	0.042
62; −46; 30	Rt. supramarginal gyrus	258	2064	5.619	<0.00001	0.042
52; 14; −28	Rt. middle temporal pole	35	280	4.843	0.00002	0.042
56; 16; 8	Rt. inferior frontal cortex (opercular part)	96	768	5.322	0.00001	0.042
52; −50; 46	Rt. inferior parietal cortex	51	408	4.681	0.00003	0.042
−8; 68; 0	Lt. superior frontal cortex (medial part)	38	304	5.274	0.00001	0.042
−14; 60; 26	Lt. superior frontal cortex	48	384	5.361	<0.00001	0.042
−38; 50; 18	Lt. middle frontal cortex	31	248	6.102	<0.00001	0.042
−56; −58; −14	Lt. inferior temporal cortex	88	704	5.176	0.00001	0.042

Results are presented at FDR$p < 0.05$ ($k > 30$). BP_{ND}, binding potential with respect to non-displaceable compartment; MNI, Montreal Neurological Institute; FDR*p*, false discovery rate-corrected *p*-value; Rt, right; Lt, left.

Table 3 Between-group comparisons of [^{11}C]ABP688 BP_{ND} seed-based resting-state functional connectivity.

Seeds	Regions	Functional connectivity (Fisher's *z*-values)			
		Patients Mean (SD)	Controls Mean (SD)	*p*-value (uncorr.)	FDR*p*
Rt. superior temporal cortex	Lt. middle frontal cortex (orbital part)	0.139 (0.176)	−0.033 (0.135)	0.0049	0.430
Rt. supramarginal gyrus	Lt. rectus	−0.053 (0.157)	−0.285 (0.212)	0.0016	0.198
Rt. inferior parietal cortex	Rt. fusiform gyrus	−0.033 (0.116)	−0.237 (0.140)	0.0001	0.016*
	Rt. inferior occipital cortex	−0.028 (0.161)	−0.225 (0.102)	0.0004	0.018*
	Lt. inferior occipital cortex	−0.039 (0.130)	−0.203 (0.096)	0.0004	0.018*
	Lt. fusiform gyrus	−0.023 (0.114)	−0.176 (0.137)	0.0020	0.062
Lt. inferior temporal cortex	Rt. precuneus	−0.072 (0.146)	0.100 (0.165)	0.0046	0.570

Results are presented at uncorrected $p < 0.005$. Asterisks indicate statistical significance at FDR$p < 0.05$.
BP_{ND}, binding potential with respect to non-displaceable compartment; SD, standard deviation; FDR*p*, false discovery rate-corrected *p*-value; Rt, right; Lt, left.

significant between-group differences in the right inferior parietal cortex seed (FDR-corrected $p < 0.05$). Compared to healthy controls, patients with major depression showed significantly less negative connectivity from the right inferior parietal cortex seed to the right fusiform gyrus (FDR-corrected $p = 0.016$), right inferior occipital cortex (FDR-corrected $p = 0.018$), and left inferior occipital cortex (FDR-corrected $p = 0.018$) (Table 3; Fig. 1(B)). When we examined the group differences in functional connectivity from the regions in which mGluR5 availability did not differ in ANCOVA shown in Supplementary Table S1, no significant group differences were found at the FDR-corrected $p < 0.05$ level (Supplementary Table S5). The [^{11}C]ABP688 BP_{ND} seed-based functional connectivity did not show significant correlations with clinical variables within the patient group. In the entire subject group, there were significant positive correlations of BDI and BHS scores with functional connectivity (FDR-corrected $p < 0.05$) (Supplementary Table S4B; Fig. 2(B)).

The strength of the functional connectivity (β-value) between the left superior medial prefrontal cortex seed and the left parahippocampal gyrus was positively correlated with the [^{11}C]ABP688 BP_{ND} in the left superior medial prefrontal cortex in the patient group ($r = 0.511$, $T = 2.23$,

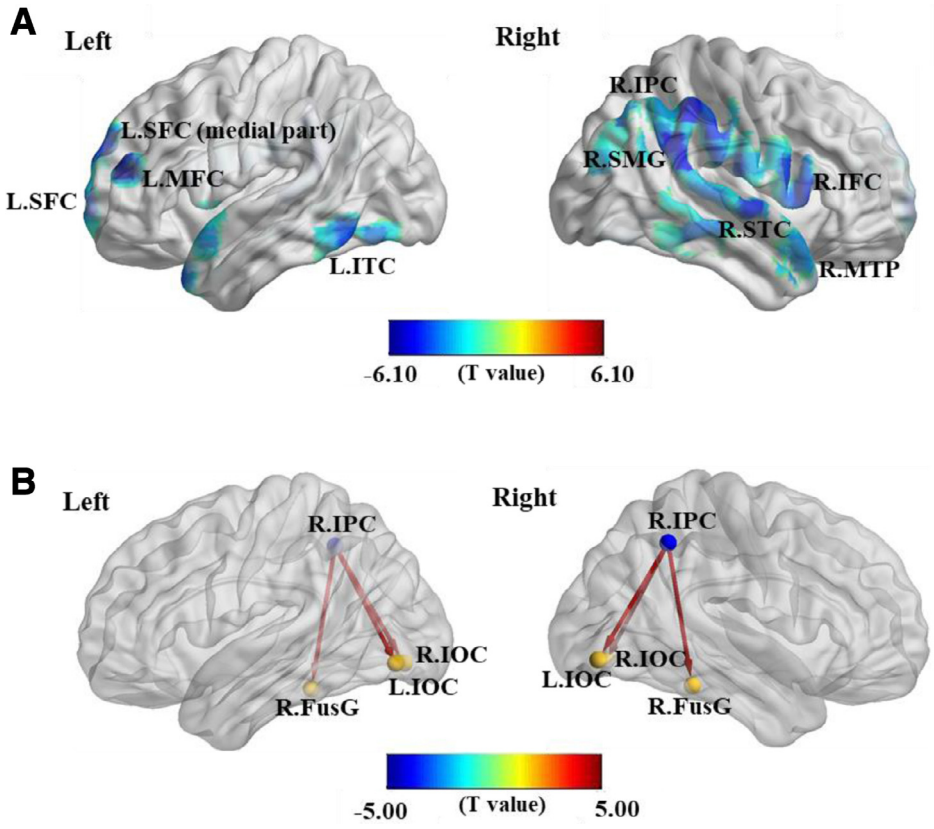

Fig. 1 Results of between-group comparisons. (A) The [^{11}C]ABP688 BP_{ND} was significantly lower in patients than in controls in clusters of voxels located in the prefrontal, temporal, and parietal cortices, and SMG (FDR$p < 0.05$). (B) The results of the between-group comparisons of [^{11}C]ABP688 BP_{ND} seed-based resting-state functional connectivity are presented at FDR$p < 0.05$. The seeds are shown as blue colored spheres. Red lines indicate significant between-group differences at FDR$p < 0.05$. Compared to healthy controls, patients showed significantly less negative connectivity from the right IPC seed to the right FusG, right IOC, and left IOC. The images were visualized with the BrainNet Viewer (http://www.nitrc.org/projects/bnv/). FDR*p*, false discovery rate-corrected *p*-value; FusG, fusiform gyrus; IFC, inferior frontal cortex; IOC, inferior occipital cortex; IPC, inferior parietal cortex; ITC; inferior temporal cortex; MFC, middle frontal cortex; MTP, middle temporal pole; SFC, superior frontal cortex; SMG, supramarginal gyrus; STC, superior temporal cortex.

$p = 0.0427$), but had a negative correlation with it in the control group ($r = -0.551$, $T = -2.38$, $p = 0.0332$), indicating significantly different patterns of associations between the groups ($p = 0.0029$) (Fig. 3; Supplementary Table S6).

4. Discussion

We quantitatively analyzed mGluR5 availability in drug-naïve young adult patients with major depression without comorbidity, using [^{11}C]ABP688 PET to examine the differences relative to healthy controls. In addition, we performed functional connectivity analyses in the same subjects to search for altered connectivity of the seed regions defined in the PET investigation. We found significantly lower mGluR5 availability in specific cortical areas in the patient group than in the control group. Furthermore, the [^{11}C]ABP688 PET seed-based rs-fMRI analysis revealed significantly less negative connectivity in the patient group. Overall, these results indicate reduced *in vivo* mGluR5 availability and related functional connectivity alterations in drug-naïve young adult patients with major depression without comorbidity.

To our knowledge, this is the first report on *in vivo* mGluR5 availability in a homogeneous group of drug-naïve young adults with major depression, and is the first combined study of mGluR5 PET and fMRI. The present study provides novel information on an integrated molecular and systems-level understanding of the pathophysiology related to depression in never-medicated young adults. Our patients were without comorbid anxiety disorders, e.g., generalized anxiety disorder, panic disorder, social phobia, and posttraumatic stress disorder, which may contribute to the relatively moderate severity of depressive symptoms in our patients. Since there was a suggestion of possible differential alteration of mGluR5 signaling in mood disorders and anxiety disorders (Esterlis et al., 2017) and previous studies may have been limited by the comorbidity, our results may shed light on the alteration of *in vivo* mGluR5 availability in depression by using a homogeneous group of subjects.

The voxel-based analysis corroborated the ROI-based finding that [^{11}C]ABP688 BP_{ND} values were significantly lower in patients than in controls in the prefrontal cortex, particularly in the anterior and ventrolateral prefrontal cor-

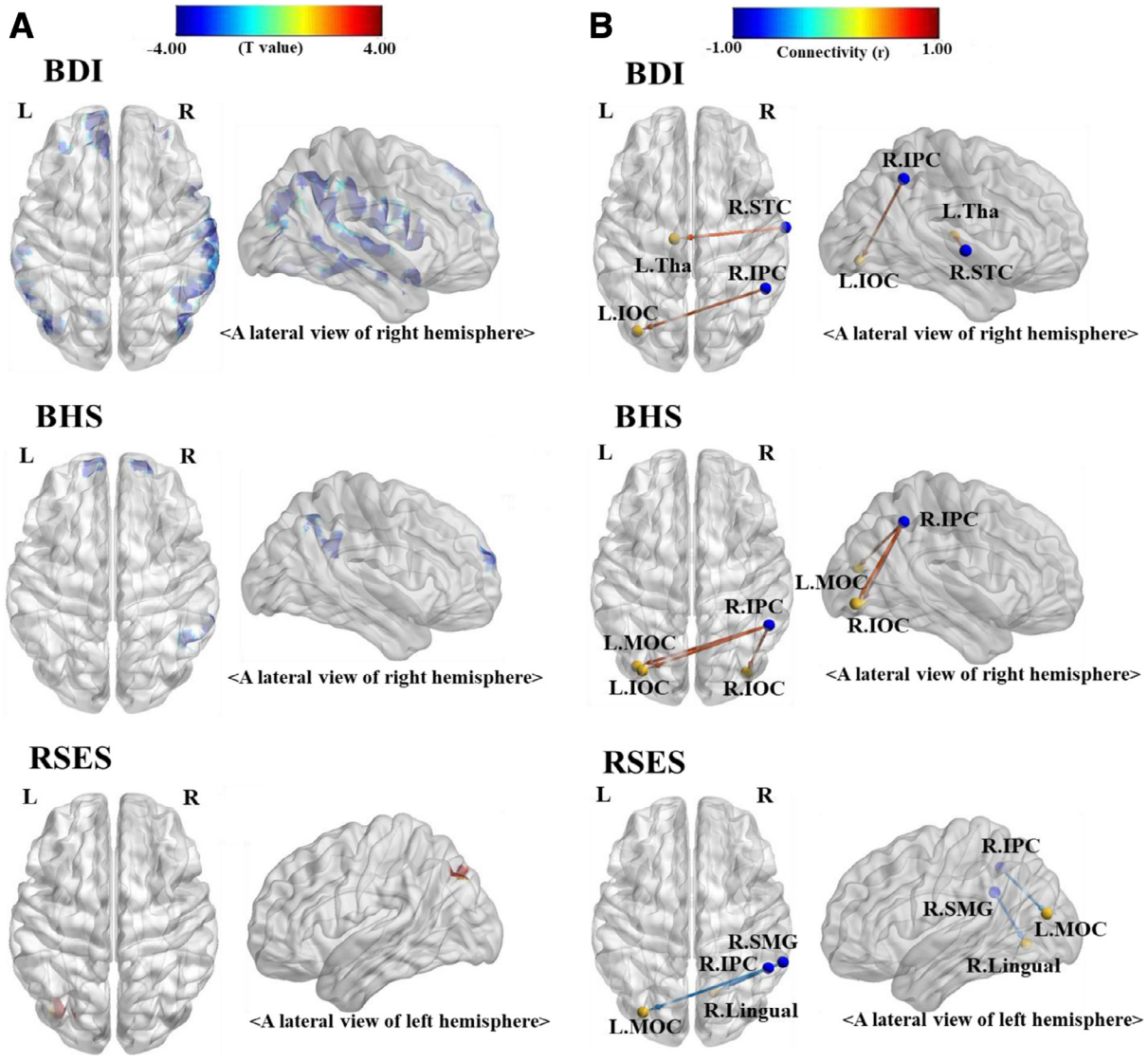

Fig. 2 Results of correlation analysis in the entire subject group ($n = 31$). (A) The results of the voxel-based analysis are presented at uncorrected $p < 0.001$. The BDI and BHS scores had negative correlations with [^{11}C]ABP688 BP_{ND}, whereas the RSES score had positive correlations with [^{11}C]ABP688 BP_{ND}. (B) The correlations between [^{11}C]ABP688 BP_{ND} seed-based functional connectivity and clinical severity are presented. The seeds are shown as blue colored spheres. Red lines indicate a positive correlation between the corresponding connectivity and the clinical variables, whereas blue lines indicate the opposite relationship. There were significant positive correlations of the BDI and BHS scores with functional connectivity (FDR$p < 0.05$), while negative correlations were found between the RSES score and functional connectivity (uncorrected $p < 0.005$). BDI, Beck Depression Inventory; BHS, Beck Hopelessness Scale; BP_{ND}, binding potential with respect to non-displaceable compartment; FDRp, false discovery rate-corrected p-value; IOC, inferior occipital cortex; IPC, inferior parietal cortex; MOC, middle occipital cortex; RSES, Rosenberg Self-Esteem Scale; SMG, supramarginal gyrus; STC, superior temporal cortex; Tha, thalamus.

tex. The voxel-based whole brain analysis also suggests the region-specific decrease in mGluR5 availability in patients with depression, mostly in higher cortical regions. Our results are generally in line with an earlier PET and post-mortem investigation (Deschwanden et al., 2011), where significantly lower levels of mGluR5 availability and protein expression in the anterior prefrontal cortex were observed, and mGluR5 availability was also lower in specific temporal and parietal cortices in patients with depression than in healthy controls. In comparison with this study, our subjects were all drug-naïve young adults without comorbidity and we employed an FDR-corrected p-value threshold in the voxel-based analysis. Notably, when we excluded smoking participants from the analysis, we found similar results in ROI-based and voxel-based analyses. Thus, the findings are attributable to depression, rather than confounding due to cigarette smoking.

Our mGluR5 PET results may lend support to the current working hypothesis of depression, which is focused on aberrant glutamatergic signaling (Sanacora et al., 2012; Haroon et al., 2017). Based on the current glutamate-mediated excitotoxicity hypothesis, an exaggerated release of

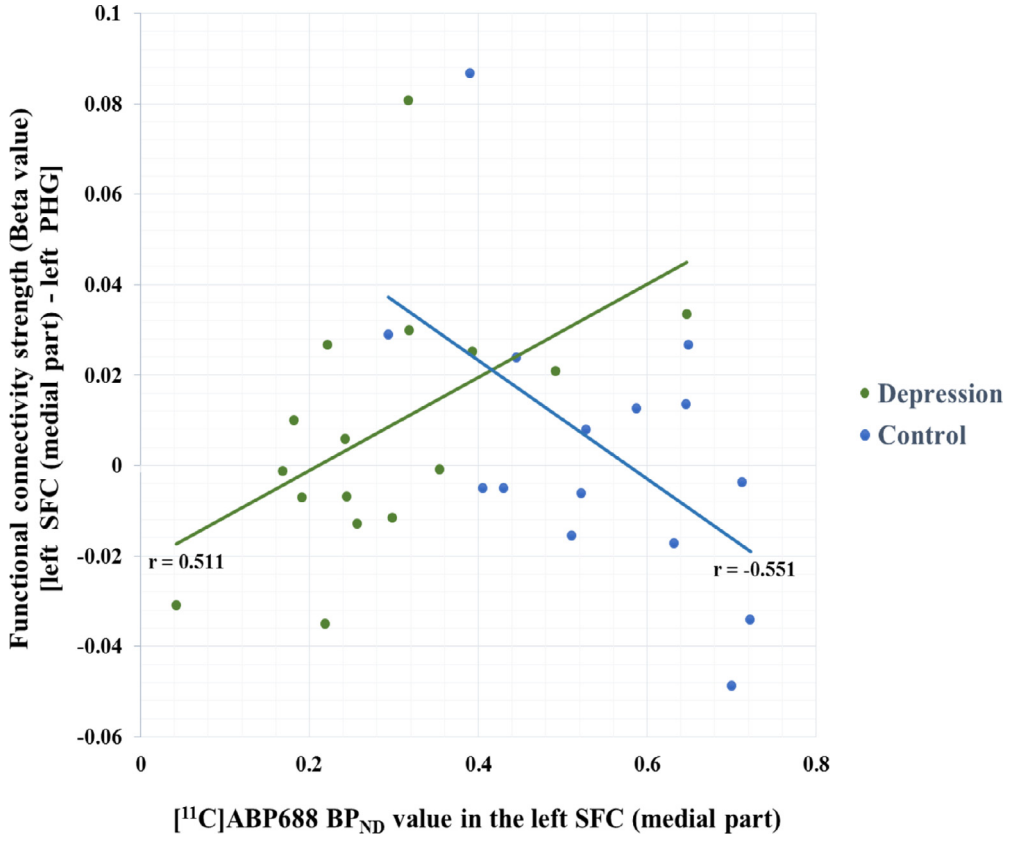

Fig. 3 Relationships between [^{11}C]ABP688 BP_{ND} and functional connectivity strength (β-value). The strength of functional connectivity (β) between the left SFC (medial part) and the left PHG, which was obtained from multivariate regression analysis, was significantly positively associated with the BP_{ND} in the left SFC (medial part) in the patient group ($p = 0.0427$), but was negatively associated with it in the control group ($p = 0.0332$), showing significantly different patterns of associations ($p = 0.0029$). BP_{ND}, binding potential with respect to non-displaceable compartment; PHG, parahippocampal gyrus; SFC, superior frontal cortex.

glutamate during immune activation leads to aberrant glutamatergic signaling in the cortical and limbic areas in patients with depression (Sanacora et al., 2012; Haroon et al., 2017). A recent study using [^{18}F]FPEB PET and magnetic resonance spectroscopy reported a significant negative correlation between *in vivo* mGluR5 availability and tissue glutamate levels, providing evidence for reduced mGluR5 availability under conditions of elevated glutamate levels (Abdallah et al., 2017). The [^{11}C]ABP688 and [^{18}F]FPEB target cell surface receptors only, and PET findings obtained using these tracers are considered to reflect neural and glial mGluR5 levels in the perisynaptic or extrasynaptic space (Esterlis et al., 2017, 2018). Therefore, our finding of significantly lower mGluR5 availability in the depression group may indicate mGluR5 internalization or downregulation due to excessive glutamate release (Esterlis et al., 2017). Alternatively, the lower mGluR5 availability may represent an inherent genetic susceptibility with increased risk of depression. Our PET findings in the prefrontal cortex may also be in accordance with the excitatory synapse hypothesis of depression (Duman, 2014; Thompson et al., 2015; Abdallah et al., 2016), in which glutamatergic synaptic dysfunction in the prefrontal cortex is held to be critically involved.

A key innovation of this study lies in our use of the [^{11}C]ABP688 PET findings to define the seed-based functional connectivity analysis using rs-fMRI data. This analysis revealed that the patient group had significantly less negative connectivity from the right inferior parietal cortex seed in which mGluR5 availability was significantly lower in patients than in controls. When we examined the group differences in functional connectivity from the regions in which mGluR5 availability did not differ, no significant group differences were observed at FDR-corrected $p < 0.05$. Overall, our results suggest a link between reduced local availability of mGluR5 and associated functional connectivity abnormalities in patients with major depression. The interpretation of reduced negative connectivity (deficient anti-correlated activity) in rs-fMRI has not been straightforward in the literature and its neurobiological meaning is a subject of debate (Chai et al., 2012; Gordon et al., 2012; Schilbach et al., 2014; Rieckmann et al., 2018). However, the less negative connectivity from the inferior parietal cortex may be in line with the recent meta-analysis result showing perturbed functional connectivity in default mode network (DMN) regions in major depression (Kaiser et al., 2015). In our study, compared to healthy controls, patients with depression showed significantly less negative connectivity from the inferior parietal cortex seed to the fusiform gyrus and inferior occipital cortex. The inferior parietal cortex is among the integral regions comprising the DMN (task-

negative network) (Cole et al., 2012), and the fusiform gyrus and inferior occipital cortex have been associated with the task-positive network (van Wingen et al., 2014; Di et al., 2014). As such, the less negative connectivity (weakened anti-correlation) between the inferior parietal cortex seed and the aforementioned regions may suggest less specific or less distinct functional network organizations in the patient group. It may also imply altered network integration and segregation in major depression, which leads to impairments in adaptive or efficient functional processing.

In our study, the correlations between mGluR5 availability and the related functional connectivity strength (β) measured by multivariate regression coefficient were opposite between the depression and control groups. This result also suggests an altered relationship between mGluR5 availability and its related functional connectivity in our drug-naïve patients with depression compared to healthy controls. This constitutes further evidence for the presence of mGluR5 availability-related functional connectivity alterations in our patients.

The present correlations with clinical severity should be interpreted with caution, since there were no significant findings when the analysis was confined to the patient group. The significant negative correlation of the BDI score with [^{11}C]ABP688 BP_{ND} in the prefrontal cortex in the entire subject group supports the findings of the between-group comparison of mGluR5 availability. In our study, all subjects underwent assessments for depressive mood, hopelessness, and self-esteem, and the direction of the correlations of these clinical ratings with mGluR5 availability was consistent in the entire subject group. Significant correlations of the BDI and BHS scores with [^{11}C]ABP688 BP_{ND} seed-based functional connectivity in entire subjects also support the finding of between-group differences in seed-based functional connectivity. Since our patients had relatively moderate depression severity, future studies should include a larger population of patients with varying degrees of depression (mild to severe) to examine the relationship between symptom severity and mGluR5-related *in vivo* imaging findings.

In this multimodal imaging study, we employed a novel combination of [^{11}C]ABP688 PET and rs-fMRI to relate molecular signaling through mGluR5 neurotransmission to functional connectivity in resting-state brain networks. We concede that the functional connectivity differences arose from a data-driven search, and do not lend themselves readily to concrete and therapeutically relevant conclusions. Our approach is new and it remains to be established how depression-related differences in mGluR5 availability could influence functional connectivity, and how this might lead to the development of specific symptoms. Additional multimodality imaging studies would be required to better understand the molecular basis of systems-level disruptions in depression.

There are certain other limitations in the interpretation of the present results. All patients were drug-naïve subjects with a median age of 22.8 years without comorbid anxiety disorders. Although this was by design, the findings may not be generalizable to a more heterogeneous group of subjects with depression. The [^{11}C]ABP688 BP_{ND} was derived using a reference tissue model, rather than the gold standard metabolite-corrected arterial input-based quantification using a two-tissue compartment (DeLorenzo et al., 2011a, 2011b). However, arterial blood sampling by cannulation of the radial artery is invasive and is associated with discomfort and potential adverse effects, which would have further limited recruitment of subjects. Moreover, imprecision in the determination of the metabolite-corrected input function can be a source of variance in compartmental analysis (Slifstein and Laruelle, 2001). In our study, BP_{ND} values were higher in the right prefrontal cortex than in the left prefrontal cortex. So far, the asymmetry of mGluR5 availability is largely unknown, although the asymmetrical involvement of mGluR5 modulation in nociceptive processing has been reported (Kolber et al., 2010). In one previous [^{11}C]ABP688 PET study of healthy subjects (DuBois et al., 2016), higher BP_{ND} was observed in the left lateral prefrontal cortex relative to the same region in the right hemisphere. Therefore, further studies with a large sample size are required to confirm the possible asymmetry of mGluR5 availability in healthy subjects and patients with major depression.

In conclusion, using a novel multimodal approach combining [^{11}C]ABP688 PET and rs-fMRI, our study provides new integrated molecular and systems-level information on the pathophysiology of depression. The results suggest lower mGluR5 availability and related functional connectivity alterations in drug-naïve young adults with major depression without comorbidity, which may underlie aspects of depressive mood and behaviors.

Conflict of interest

The authors declare no conflict of interest.

Contributors

Jong-Hoon Kim conceived the study design, recruited subjects, and carried out data analysis, interpretation, and manuscript writing. Yo-Han Joo, Jeong-Hee Kim, and Yun-Kwan Kim carried out PET/MRI scanning, data acquisition and analysis, and contributed to drafting the manuscript. Sang-Yoon Lee synthesized radiotracers, carried out PET imaging, and contributed to drafting the manuscript. Young-Don Son and Hang-Keun Kim, and Tatsuo Ido carried out data analysis and interpretation, and contributed to manuscript writing. All authors have read and approved the final manuscript.

Acknowledgments

This research was supported by the Brain Research Program through the National Research Foundation of Korea (NRF) funded by the Ministry of Science, ICT & Future Planning (2016M3C7A1914451) and by a grant of the Korean Health Technology R&D Project, Ministry of Health & Welfare (MoHW), Republic of Korea (number: HI14C2750). The NRF

and MoHW had no further role in study design; in the collection, analysis and interpretation of data; in the writing of the report; and in the decision to submit the paper for publication. We thank all the participants who took part in this study, and Jee-Eun Jeon for her research coordination. We thank Inglewood Biomedical Imaging for valuable help in manuscript editing.

Supplementary materials

Supplementary material associated with this article can be found, in the online version, at doi:10.1016/j.euroneuro.2018.12.001.

References

Aalto-Setälä, T., Marttunen, M., Tuulio-Henriksson, A., Poikolainen, K., Lönnqvist, J., 2001. One-month prevalence of depression and other DSM-IV disorders among young adults. Psychol. Med. 31, 791–801.

Abdallah, C.G., Sanacora, G., Duman, R.S., Krystal, J.H., 2015. Ketamine and rapid-acting antidepressants: a window into a new neurobiology for mood disorder therapeutics. Annu. Rev. Med. 66, 509–523.

Abdallah, C.G., Adams, T.G., Kelmendi, B., Esterlis, I., Sanacora, G., Krystal, J.H., 2016. Ketamine's mechanism of action: a path to rapid-acting antidepressants. Depress. Anxiety 33, 689–697.

Abdallah, C.G., Hannestad, J., Mason, G.F., Holmes, S.E., Della-Gioia, N., Sanacora, G., Jiang, L., Matuskey, D., Satodiya, R., Gasparini, F., Lin, X., Javitch, J., Planeta, B., Nabulsi, N., Carson, R.E., Esterlis, I., 2017. Metabotropic glutamate receptor 5 and glutamate involvement in major depressive disorder: a multimodal imaging study. Biol. Psychiatry Cognit. Neurosci. Neuroimaging 2, 449–456.

Abi-Dargham, A., Horga, G., 2016. The search for imaging biomarkers in psychiatric disorders. Nat. Med. 22, 1248–1255.

Akkus, F., Ametamey, S.M., Treyer, V., Burger, C., Johayem, A., Umbricht, D., Gomez Mancilla, B., Sovago, J., Buck, A., Hasler, G., 2013. Marked global reduction in mGluR5 receptor binding in smokers and ex-smokers determined by [^{11}C]ABP688 positron emission tomography. Proc. Natl. Acad. Sci. U.S.A. 110, 737–742.

American Psychiatric Association, 1994. Diagnostic and Statistical Manual of Mental Disorders: DSM-IV, fourth ed. American Psychiatric Association, Washington, DC.

Ametamey, S.M., Kessler, L.J., Honer, M., Wyss, M.T., Buck, A., Hintermann, S., Auberson, Y.P., Gasparini, F., Schubiger, P.A., 2006. Radiosynthesis and preclinical evaluation of ^{11}C-ABP688 as a probe for imaging the metabotropic glutamate receptor subtype 5. J. Nucl. Med. 47, 698–705.

Anand, A., Li, Y., Wang, Y., Wu, J., Gao, S., Bukhari, L., Mathews, V.P., Kalnin, A., Lowe, M.J., 2005. Activity and connectivity of brain mood regulating circuit in depression: a functional magnetic resonance study. Biol. Psychiatry 57, 1079–1088.

Beck, A.T., 1967. Depression: Clinical, Experimental, and Theoretical Aspects. Harper & Row, New York.

Beck, A.T., Weissman, A., Lester, D., Trexler, L., 1974. The measurement of pessimism: the hopelessness scale. J. Consult. Clin. Psychol. 42, 861–865.

Behzadi, Y., Restom, K., Liau, J., Liu, T.T., 2007. A component based noise correction method (CompCor) for BOLD and perfusion based fMRI. NeuroImage 37, 90–101.

Belozertseva, I.V., Kos, T., Popik, P., Danysz, W., Bespalov, A.Y., 2007. Antidepressant-like effects of mGluR1 and mGluR5 antagonists in the rat forced swim and the mouse tail suspension tests. Eur. Neuropsychopharmacol. 17, 172–179.

Berthele, A., Platzer, S., Laurie, D.J., Weis, S., Sommer, B., Zieglgänsberger, W., Conrad, B., Tölle, T.R., 1999. Expression of metabotropic glutamate receptor subtype mRNA (mGluR1-8) in human cerebellum. Neuroreport 10, 3861–3867.

Bradbury, M.J., Giracello, D.R., Chapman, D.F., Holtz, G., Schaffhauser, H., Rao, S.P., Varney, M.A., Anderson, J.J., 2003. Metabotropic glutamate receptor 5 antagonist-induced stimulation of hypothalamic-pituitary-adrenal axis activity: interaction with serotonergic systems. Neuropharmacology 44, 562–572.

Chai, X.J., Castañón, A.N., Ongür, D., Whitfield-Gabrieli, S., 2012. Anticorrelations in resting state networks without global signal regression. NeuroImage 59, 1420–1428.

Chaki, S., Ago, Y., Palucha-Paniewiera, A., Matrisciano, F., Pilc, A., 2013. mGlu2/3 and mGlu5 receptors: potential targets for novel antidepressants. Neuropharmacology 66, 40–52.

Chowdhury, G.M., Zhang, J., Thomas, M., Banasr, M., Ma, X., Pittman, B., Bristow, L., Schaeffer, E., Duman, R.S., Rothman, D.L., Behar, K.L., Sanacora, G., 2017. Transiently increased glutamate cycling in rat PFC is associated with rapid onset of antidepressant-like effects. Mol. Psychiatry 22, 120–126.

Cole, D.M., Beckmann, C.F., Searle, G.E., Plisson, C., Tziortzi, A.C., Nichols, T.E., Gunn, R.N., Matthews, P.M., Rabiner, E.A., Beaver, J.D., 2012. Orbitofrontal connectivity with resting-state networks is associated with midbrain dopamine D3 receptor availability. Cereb. Cortex 22, 2784–2793.

Daggett, L.P., Sacaan, A.I., Akong, M., Rao, S.P., Hess, S.D., Liaw, C., Urrutia, A., Jachec, C., Ellis, S.B., Dreessen, J., Knöpfel, T., Landwehrmeyer, G.B., Testa, C.M., Young, A.B., Varney, M., Johnson, E.C., Veliçelebi, G., 1995. Molecular and functional characterization of recombinant human metabotropic glutamate receptor subtype 5. Neuropharmacology 34, 871–886.

DeLorenzo, C., Kumar, J.S., Mann, J.J., Parsey, R.V., 2011a. In vivo variation in metabotropic glutamate receptor subtype 5 binding using positron emission tomography and [^{11}C]ABP688. J. Cereb. Blood Flow Metab. 31, 2169–2180.

DeLorenzo, C., Milak, M.S., Brennan, K.G., Kumar, J.S., Mann, J.J., Parsey, R.V., 2011b. In vivo positron emission tomography imaging with [^{11}C]ABP688: binding variability and specificity for the metabotropic glutamate receptor subtype 5 in baboons. Eur. J. Nucl. Med. Mol. Imaging 38, 1083–1094.

DeLorenzo, C., Sovago, J., Gardus, J., Xu, J., Yang, J., Behrje, R., Kumar, J.S., Devanand, D.P., Pelton, G.H., Mathis, C.A., Mason, N.S., Gomez-Mancilla, B., Aizenstein, H., Mann, J.J., Parsey, R.V., 2015. Characterization of brain mGluR5 binding in a pilot study of late-life major depressive disorder using positron emission tomography and [^{11}C]ABP688. Transl. Psychiatry 5, e693.

DeLorenzo, C., Gallezot, J.D., Gardus, J., Yang, J., Planeta, B., Nabulsi, N., Ogden, R.T., Labaree, D.C., Huang, Y.H., Mann, J.J., Gasparini, F., Lin, X., Javitch, J.A., Parsey, R.V., Carson, R.E., Esterlis, I., 2017. In vivo variation in same-day estimates of metabotropic glutamate receptor subtype 5 binding using [(11)C]ABP688 and [(18)F]FPEB. J. Cereb. Blood Flow Metab. 37, 2716–2727.

Deschwanden, A., Karolewicz, B., Feyissa, A.M., Treyer, V., Ametamey, S.M., Johayem, A., Burger, C., Auberson, Y.P., Sovago, J., Stockmeier, C.A., Buck, A., Hasler, G., 2011. Reduced metabotropic glutamate receptor 5 density in major depression determined by [(11)C]ABP688 PET and postmortem study. Am. J. Psychiatry 168, 727–734.

Di, X., Kim, E.H., Chen, P., Biswal, B.B., 2014. Lateralized resting-state functional connectivity in the task-positive and task-negative networks. Brain Connect 4, 641–648.

DuBois, J.M., Rousset, O.G., Rowley, J., Porras-Betancourt, M., Reader, A.J., Labbe, A., Massarweh, G., Soucy, J.P., Rosa-Neto, P., Kobayashi, E., 2016. Characterization of age/sex and the regional distribution of mGluR5 availability in the healthy human brain measured by high-resolution [(11)C]ABP688 PET. Eur. J. Nucl. Med. Mol. Imaging 43, 152–162.

Duman, R.S., 2014. Neurobiology of stress, depression, and rapid acting antidepressants: remodeling synaptic connections. Depress. Anxiety 31, 291–296.

Elmenhorst, D., Minuzzi, L., Aliaga, A., Rowley, J., Massarweh, G., Diksic, M., Bauer, A., Rosa-Neto, P., 2010. In vivo and in vitro validation of reference tissue models for the mGluR(5) ligand [(11)C]ABP688. J. Cereb. Blood Flow Metab. 30, 1538–1549.

Esterlis, I., Holmes, S.E., Sharma, P., Krystal, J.H., DeLorenzo, C., 2017. Metabotropic glutamatergic receptor 5 and stress disorders: knowledge gained from receptor imaging studies. Biol. Psychiatry doi:10.1016/j.biopsych.2017.08.025.

Esterlis, I., DellaGioia, N., Pietrzak, R.H., Matuskey, D., Nabulsi, N., Abdallah, C.G., Yang, J., Pittenger, C., Sanacora, G., Krystal, J.H., Parsey, R.V., Carson, R.E., DeLorenzo, C., 2018. Ketamine-induced reduction in mGluR5 availability is associated with an antidepressant response: an [(11)C]ABP688 and PET imaging study in depression. Mol. Psychiatry 23, 824–832.

First, M.B., Spitzer, R.L., Gibbon, M., Williams, J.B.W., 1996. Structured Clinical Interview for DSM-IV Axis I Disorders Research Version (SCID-I). New York State Psychiatric Institute Biometrics Research, New York.

Gordon, E.M., Stollstorff, M., Devaney, J.M., Bean, S., Vaidya, C.J., 2012. Effect of dopamine transporter genotype on intrinsic functional connectivity depends on cognitive state. Cereb. Cortex 22, 2182–2196.

Grimm, S., Beck, J., Schuepbach, D., Hell, D., Boesiger, P., Bermpohl, F., Niehaus, L., Boeker, H., Northoff, G., 2008. Imbalance between left and right dorsolateral prefrontal cortex in major depression is linked to negative emotional judgment: an fMRI study in severe major depressive disorder. Biol Psychiatry 63, 369–376.

Guo, W., Liu, F., Xue, Z., Gao, K., Liu, Z., Xiao, C., Chen, H., Zhao, J., 2013. Abnormal resting-state cerebellar-cerebral functional connectivity in treatment-resistant depression and treatment sensitive depression. Prog. Neuropsychopharmacol. Biol. Psychiatry 44, 51–57.

Hamilton, M., 1960. A rating scale for depression. J. Neurol. Neurosurg. Psychiatry 23, 56–62.

Haroon, E., Miller, A.H., Sanacora, G., 2017. Inflammation, glutamate, and glia: a trio of trouble in mood disorders. Neuropsychopharmacology 42, 193–215.

Hulka, L.M., Treyer, V., Scheidegger, M., Preller, K.H., Vonmoos, M., Baumgartner, M.R., Johayem, A., Ametamey, S.M., Buck, A., Seifritz, E., Quednow, B.B., 2014. Smoking but not cocaine use is associated with lower cerebral metabotropic glutamate receptor 5 density in humans. Mol. Psychiatry 19, 625–632.

Hwang, J.W., Xin, S.C., Ou, Y.M., Zhang, W.Y., Liang, Y.L., Chen, J., Yang, X.Q., Chen, X.Y., Guo, T.W., Yang, X.J., Ma, W.H., Li, J., Zhao, B.C., Tu, Y., Kong, J., 2016. Enhanced default mode network connectivity with ventral striatum in subthreshold depression individuals. J. Psychiatr. Res. 76, 111–120.

Hyder, F., Kida, I., Behar, K.L., Kennan, R.P., Maciejewski, P.K., Rothman, D.L., 2001. Quantitative functional imaging of the brain: towards mapping neuronal activity by BOLD fMRI. NMR Biomed. 14, 413–431.

Ibrahim, A.K., Kelly, S.J., Adams, C.E., Glazebrook, C., 2013. A systematic review of studies of depression prevalence in university students. J. Psychiatr. Res. 47, 391–400.

Kaiser, R.H., Andrews-Hanna, J.R., Wager, T.D., Pizzagalli, D.A., 2015. Large-scale network dysfunction in major depressive disorder: a meta-analysis of resting-state functional connectivity. JAMA Psychiatry 72, 603–611.

Kaiser, R.H., Whitfield-Gabrieli, S., Dillon, D.G., Goer, F., Beltzer, M., Minkel, J., Smoski, M., Dichter, G., Pizzagalli, D.A., 2016. Dynamic resting-state functional connectivity in major depression. Neuropsychopharmacology 41, 1822–1830.

Kida, I., Hyder, F., 2006. Physiology of functional magnetic resonance imaging: energetics and function. Methods Mol. Med. 124, 175–195.

Kolber, B.J., Montana, M.C., Carrasquillo, Y., Xu, J., Heinemann, S.F., Muglia, L.J., Gereau, R.W.4th., 2010. Activation of metabotropic glutamate receptor 5 in the amygdala modulates pain-like behavior. J. Neurosci. 30, 8203–8213.

Lancaster, J.L., Woldorff, M.G., Parsons, L.M., Liotti, M., Freitas, C.S., Rainey, L., Kochunov, P.V., Nickerson, D., Mikiten, S.A., Fox, P.T., 2000. Automated Talairach atlas labels for functional brain mapping. Hum. Brain Mapp. 10, 120–131.

Legutko, B., Szewczyk, B., Pomierny-Chamioło, L., Nowak, G., Pilc, A., 2006. Effect of MPEP treatment on brain-derived neurotrophic factor gene expression. Pharmacol. Rep. 58, 427–430.

Li, X., Need, A.B., Baez, M., Witkin, J.M., 2006. Metabotropic glutamate 5 receptor antagonism is associated with antidepressant-like effects in mice. J. Pharmacol. Exp. Ther. 319, 254–259.

Liu, L., Zeng, L.L., Li, Y., Ma, Q., Li, B., Shen, H., Hu, D., 2012. Altered cerebellar functional connectivity with intrinsic connectivity networks in adults with major depressive disorder. PLoS One 7, e39516.

Martinot, J.L., Hardy, P., Feline, A., Huret, J.D., Mazoyer, B., Attar-Levy, D., Pappata, S., Syrota, A., 1990. Left prefrontal glucose hypometabolism in the depressed state: a confirmation. Am. J. Psychiatry 147, 1313–1317.

Mathews, W.B., Kuwabara, H., Stansfield, K., Valentine, H., Alexander, M., Kumar, A., Hilton, J., Dannals, R.F., Wong, D.F., Gasparini, F., 2014. Dose-dependent, saturable occupancy of the metabotropic glutamate subtype 5 receptor by fenobam as measured with [(11)C]ABP688 PET imaging. Synapse doi:10.1002/syn.21775.

Ochsner, K.N., Bunge, S.A., Gross, J.J., Gabrieli, J.D., 2002. Rethinking feelings: an FMRI study of the cognitive regulation of emotion. J. Cognit. Neurosci. 14, 1215–1229.

Paillère Martinot, M.L., Galinowski, A., Ringuenet, D., Gallarda, T., Lefaucheur, J.P., Bellivier, F., Picq, C., Bruguière, P., Mangin, J.F., Rivière, D., Willer, J.C., Falissard, B., Leboyer, M., Olié, J.P., Artiges, E., Martinot, J.L., 2010. Influence of prefrontal target region on the efficacy of repetitive transcranial magnetic stimulation in patients with medication-resistant depression: a [(18)F]-fluorodeoxyglucose PET and MRI study. Int. J. Neuropsychopharmacol. 13, 45–59.

Rieckmann, A., Johnson, K.A., Sperling, R.A., Buckner, R.L., Hedden, T., 2018. Dedifferentiation of caudate functional connectivity and striatal dopamine transporter density predict memory change in normal aging. Proc. Natl. Acad. Sci. U.S.A. 115, 10160–10165.

Rosenberg, M., 1965. Society and the Adolescent Self-Image. Princeton University Press, Princeton.

Sanacora, G., Treccani, G., Popoli, M., 2012. Towards a glutamate hypothesis of depression: an emerging frontier of neuropsychopharmacology for mood disorders. Neuropharmacology 62, 63–77.

Sanacora, G., Frye, M.A., McDonald, W., Mathew, S.J., Turner, M.S., Schatzberg, A.F., Summergrad, P., Nemeroff, C.B., 2017. A consensus statement on the use of ketamine in the treatment of mood disorders. JAMA Psychiatry 74, 399–405.

Schilbach, L., Müller, V.I., Hoffstaedter, F., Clos, M., Goya-Maldonado, R., Gruber, O., Eickhoff, S.B., 2014. Meta-analytically informed network analysis of resting state FMRI reveals hyperconnectivity in an introspective socio-affective network in depression. PLoS One 23, e94973.

Singh, J.B., Fedgchin, M., Daly, E.J., De Boer, P., Cooper, K., Lim, P., Pinter, C., Murrough, J.W., Sanacora, G., Shelton, R.C., Kurian, B., Winokur, A., Fava, M., Manji, H., Drevets, W.C., Van Nueten, L., 2016. A double-blind, randomized, placebo-controlled, dose-frequency study of intravenous ketamine in patients with treatment-resistant depression. Am. J. Psychiatry 173, 816–826.

Slifstein, M., Laruelle, M., 2001. Models and methods for derivation of *in vivo* neuroreceptor parameters with PET and SPECT reversible radiotracers. Nucl. Med. Biol. 28, 595–608.

Smolders, I., Clinckers, R., Meurs, A., De Bundel, D., Portelli, J., Ebinger, G., Michotte, Y., 2008. Direct enhancement of hippocampal dopamine or serotonin levels as a pharmacodynamic measure of combined antidepressant-anticonvulsant action. Neuropharmacology 54, 1017–1028.

Tatarczyńska, E., Klodzińska, A., Chojnacka-Wójcik, E., Palucha, A., Gasparini, F., Kuhn, R., Pilc, A., 2001. Potential anxiolytic- and antidepressant-like effects of MPEP, a potent, selective and systemically active mGlu5 receptor antagonist. Br. J. Pharmacol. 132, 1423–1430.

Teffer, K., Semendeferi, K., 2012. Human prefrontal cortex: evolution, development, and pathology. Prog. Brain Res. 195, 191–218.

Thompson, S.M., Kallarackal, A.J., Kvarta, M.D., Van Dyke, A.M., LeGates, T.A., Cai, X., 2015. An excitatory synapse hypothesis of depression. Trends Neurosci. 38, 279–294.

Tu, J.C., Xiao, B., Naisbitt, S., Yuan, J.P., Petralia, R.S., Brakeman, P., Doan, A., Aakalu, V.K., Lanahan, A.A., Sheng, M., Worley, P.F., 1999. Coupling of mGluR/Homer and PSD-95 complexes by the Shank family of postsynaptic density proteins. Neuron 23, 583–592.

Tzourio-Mazoyer, N., Landeau, B., Papathanassiou, D., Crivello, F., Etard, O., Delcroix, N., Mazoyer, B., Joliot, M., 2002. Automated anatomical labeling of activations in SPM using a macroscopic anatomical parcellation of the MNI MRI single-subject brain. NeuroImage 15, 273–289.

van Wingen, G.A., Tendolkar, I., Urner, M., van Marle, H.J., Denys, D., Verkes, R.J., Fernández, G., 2014. Short-term antidepressant administration reduces default mode and task-positive network connectivity in healthy individuals during rest. NeuroImage 88, 47–53.

Whitfield-Gabrieli, S., Nieto-Castanon, A., 2012. Conn: a functional connectivity toolbox for correlated and anticorrelated brain networks. Brain Connect 2, 125–141.

Wu, Y., Carson, R.E., 2002. Noise reduction in the simplified reference tissue model for neuroreceptor functional imaging. J. Cereb. Blood Flow Metab. 22, 1440–1452.

Zarate Jr., C.A., Singh, J.B., Carlson, P.J., Brutsche, N.E., Ameli, R., Luckenbaugh, D.A., Charney, D.S., Manji, H.K., 2006. A randomized trial of an N-methyl-D-aspartate antagonist in treatment-resistant major depression. Arch. Gen. Psychiatry 63, 856–864.

Zhou, Y., Yu, C., Zheng, H., Liu, Y., Song, M., Qin, W., Li, K., Jiang, T., 2010. Increased neural resources recruitment in the intrinsic organization in major depression. J. Affect. Disord. 121, 220–230.

Zimmerman, M., Martinez, J.H., Young, D., Chelminski, I., Dalrymple, K., 2013. Severity classification on the Hamilton Depression Rating Scale. J. Affect. Disord. 150, 384–388.